Liu *et al. Journal of Ovarian Research* (2025) 18:7
https://doi.org/10.1186/s13048-025-01587-5

Journal of Ovarian Research

RESEARCH Open Access

Woxuanzhongzhou formula improves DHEAS and high-fat diet-induced IR and anovulatory mice via AMPK/PGC1- α/Irisin pathway

Haijuan Liu[1,2], Guohua Wang[1*], Conglu Sui[1*], Yanan Guo[1] and Xiangyu He[3]

Abstract

Background Polycystic ovary syndrome (PCOS) is a common endocrine and metabolic disorder in women of reproductive age. Anovulation is one of the most important clinical features of PCOS, and insulin resistance (IR) is one of the critical pathogenic factors. Woxuanzhongzhou (WXZZ) is a traditional herbal formulation that has shown efficacy in treating PCOS combined with IR, but the underlying mechanism is not clear. The aim of this study was to investigate the molecular mechanism of WXZZ on dehydroepiandrosterone sulfate and high fat diet induced PCOS with IR mice.

Methods 40 female C57BL/6 mice were randomized to 4 groups: control group, model group, metformin group, and WXZZ group. Some mice is induced by dehydroepiandrosterone sulfate (DHEA) and high-fat diet (HFD) for 3 weeks. Following model induction, metformin and WXZZ were administered by gavage. Body weight, fasting blood glucose (FBG), fasting insulin (FINS) levels, the homeostatic model assessment of insulin resistance (HOMA-IR), and gonadal hormones were measured. Estrous cycles were monitored. The structure of the gastrocnemius muscle and subcutaneous fatty tissue were also evaluated. Additionally, serum irisin and non-esterified fatty acids (NEAF) levels and the protein and gene expression levels of AMPK, PGC1-α, FNDC5, irisin in the gastrocnemius muscle and CaMKK, AMPK, PGC1-α, UCP1 in fat were analyzed.

Results The DHEA + HFD + WXZZ group exhibited significant improvements in several key parameters compared to the DHEA + HFD group. WXZZ ameliorated endocrine and metabolic disorders, resumed estrous cycle in DHEAS and high-fat diet-induced IR and anovulatory mice. Significant reductions were observed in body weight, serum testosterone, luteinizing hormone, luteinizing hormone/ follicle-stimulating hormone ratio, FINS, and HOMA-IR. Additionally, WXZZ promoted irisin expression and secretion by up-regulating the protein and gene AMPK/PGC1-α/FNDC5 expression in gastrocnemius muscle and up-regulated the protein and gene CaMKK/AMPK/PGC1-α/UCP1 expression in fat. WXZZ inhibited the overproduction of serum NEFA, and reduced lipid accumulation. Structural analysis of the gastrocnemius muscle and adipose tissue revealed partial restoration.

*Correspondence:
Guohua Wang
wgh1188@163.com
Conglu Sui
suiconglu@126.com

Full list of author information is available at the end of the article

Conclusion WXZZ exhibits therapeutic effects in DHEAS and high-fat diet-induced IR and anovulatory mice. These effects may be mediated through the activation of AMPK/PGC1-α pathway in muscle to promote the secretion of irisin.

Keywords Polycystic ovary syndrome, Insulin resistance, Irisin, FNDC5, AMPK, PGC1-α

Introduction

Polycystic ovary syndrome (PCOS) is a prevalent endocrine and metabolic disorder affecting approximately 5-20% of women of reproductive age globally [1]. Characterized by hyperandrogenism, ovulatory dysfunction, and polycystic ovarian morphology, PCOS is also strongly associated with metabolic disturbances including insulin resistance (IR), obesity, and type 2 diabetes mellitus [2]. IR, a hallmark of PCOS, exacerbates reproductive and metabolic anomalies, creating a vicious cycle that hampers effective management of the syndrome. Approximately 35-80% of PCOS patients combined with IR [3], up to 80% of PCOS patients exhibit IR independent of body mass index (BMI) [4].

Adipose tissue-derived hormones and myokines play a crucial role in regulating metabolic balance. One such myokine is irisin, which is mainly produced in skeletal muscle in response to physical exercise [5]. Irisin has various biological functions [6] and shows 100% similarity between rats and humans [7]. Notably, serum levels of irisin have been associated with hyperandrogenism [8, 9], a key clinical feature of PCOS, and have shown a strong correlation with metabolic disorders, including IR and obesity in patients with PCOS [10]. Irisin is released by the proteolytic cleavage of fibronectin type III domain-containing protein 5 (FNDC5) which is regulated by peroxisome proliferator-activated receptor gamma coactivator-1 alpha (PGC-1α) [11]. PGC-1α is another critical regulator of cellular energy metabolism. It acts as a transcriptional coactivator that modulates multiple metabolic pathways including mitochondrial biogenesis and oxidative phosphorylation [12]. Adenosine monophosphate-activated protein kinase (AMPK) is an upstream regulator of PGC-1α, which plays a key role in regulating glucose and lipid metabolism, thereby impacting insulin sensitivity [13–15].

The initial understanding of nature noumenon in ancient China philosophy was based on "Qi". It refers to a universal vital energy responsible for various life processes [16]. Qi has three meanings in philosophy: first, qi is the origin of the material world, and all things are composed of qi; second, qi has two attributes of yin and yang, yin refers to tangible things, and yang is invisible; third, qi is constantly moving and changing, and its forms are ascending and descending, entering and exiting, circulating and transforming [17]. The fundamental attribute of qi is movement change [18]. Yin and Yang constitute the basic concepts of China philosophy. As opposed and complementary conditions, they symbolize the concept of dynamic equilibrium [19]. PCOS is characterized by Yin essence not waiting for full bloom in early follicular stage, and part of "Yin" is transformed into "Yang" in advance, forming the trend of "Yin not abundant-Yang first arriving", wasting Yin essence, delaying the overall unification of Yang and affecting follicular development and ovulation [20]. This imbalance of Yin and Yang is the key to the pathogenesis of ovulation disorder in PCOS [20], and affects the endocrine system leading to irregular menstruation, and affects the metabolic system impairing glucose tolerance, insulin resistance and dyslipidemia [21].

In our previous clinical trial, we have demonstrated the effect of a traditional herbal formulation called WoXuan-ZhongZhou (WXZZ) in treating patients with PCOS-IR. WXZZ significantly improved waist-to-hip ratio (WHR), BMI, homeostatic model assessment of insulin resistance (HOMA-IR), luteinizing hormone/ follicle - stimulating hormone (LH/FSH), and cholesterol level [22]. However, the molecular mechanism of this intervention is still unclear. Previous studies have suggested that irisin can alleviate ovarian fibrosis [23], and improved the motility cycle with reducing levels of testosterone (T), anti-mullerian hormone (AMH), LH, LH/FSH ratio in mice with PCOS. Thus, we aimed to investigates the hypothesis that WXZZ alleviates PCOS-IR through modulation of the AMPK-PGC-1α-irisin pathway.

Materials and methods

Chemicals and reagents

The WXZZ decoction (Beijing Kangrentang Pharmaceutical Co., Ltd., China) was dissolved in heated (60 °C) deionized water to obtain a 3.0 g/mL stock solution and stored at 4 °C. Metformin was purchased from Zhongmei Shanghai Squibb Pharmaceutical Co., Ltd. Dehydroepiandrosterone sulfate (DHEA) was purchased from Beijing Abifan Biotechnology Co., Ltd.

Animal

SPF-grade female C57BL/6 mice, aged 3 weeks and weighing 10–12 g, were obtained from Spivey Biotechnology Co., Ltd (Beijing, China). Upon arrival, the animals were housed in the Animal Experiment Center of Beijing University of Chinese Medicine. A total of 40 mice were randomly assigned to 8 cages, with 5 mice per cage. The animals were maintained under controlled environmental conditions, with a room temperature of

20–25 °C, relative humidity of 40–60%, and a 12-hour light/dark cycle. Food and water were provided ad libitum.

All experimental procedures involving animals were reviewed and approved by the Laboratory Animal Ethics Sub-committee of the Academic Committee of Beijing University of Chinese Medicine (Approval No. BUCM-2023030104-1105).

DHEAS and high-fat diet-induced IR and anovulatory mice

Animals were randomly assigned to control or experimental group. IR and anovulatory mice model was induced by DHEA and high-fat diet (HFD) [24].The experimental group ($n = 30$) was subjected to a daily subcutaneous injection of 0.2 mL DHEA (6 mg/kg) [24], administered into the dorsal neck region. The DHEA was prepared in a solution with soybean oil. In addition, these animals were fed a HFD (4.73 kcal/g; Beijing Huafukang Biotechnology Co., Ltd.), with an energy distribution of 20% protein, 35% carbohydrate, and 45% fat. The control group ($n = 10$) received an equivalent subcutaneous injection of 0.2 mL soybean oil, administered under identical conditions, and were fed a standard diet (3.85 kcal/g; Beijing Huafukang Biotechnology Co., Ltd.) with an energy distribution of 20% protein, 70% carbohydrate, and 10% fat.

The injections and diet regimen were administered continuously for 3 weeks. Throughout the study, all animals were weighed daily at approximately 8:00 a.m. by the same researcher who recorded using an electronic balance, with measurements expressed in grams. Vaginal smears were collected daily at approximately 9:00 a.m. for 12 consecutive days, starting from the 10th day of the modeling phase. The collected cells were preserved using 4% paraformaldehyde fixation to ensure optimal preservation of cellular morphology for subsequent analysis of estrous cycle.

At the end of the treatment period, animals were fasted for 12 h, with only water provided, before blood collection. Fasting blood glucose (FBG) levels were measured using blood obtained from the tail vein. Following this, blood was collected from the retro-orbital sinus under anesthesia to separate serum for the determination of fasting insulin (FINS) levels and gonadal hormones. Then 7 mice (3 in the control group and 4 in the model group) were killed by cervical decertification method to observe the structural changes of ovarian tissue, so as to ensure the successful establishment of PCOS mouse model.

Insulin resistance in this study was evaluated using HOMA-IR [25]. The HOMA-IR index was calculated using the formula:

$$\text{Home} - \text{IR} = \frac{\text{FBG(mmol/L)} \times \text{FINS(mU/L)}}{22.5}$$

The mice model was defined as a significant increase in body weight, serum T, and LH levels compared to the control group, along with vaginal smears showing abnormal estrous cycle and increasing ovarian follicles. Additionally, a HOMA-IR index should exceed 1.96 standard deviations above the mean of the control group.

Table 1 Characteristics of vaginal exfoliated cells in different estrous cycles

stage	characteristics of vaginal exfoliated cells
proestrus	predominantly oval nucleated epithelial cells with fewer leukocytes and keratinized epithelial cells
estrus	keratinized epithelial cells predominate, with fewer leukocytes and nucleated epithelial cells.
metestrus	the distribution of keratinized epithelial cells, nucleated epithelial cells and leukocytes was relatively balanced and not significantly different.
diestrus	predominantly leukocytes with fewer nucleated and keratinized epithelial cells .

Experimental grouping and treatment

Mice in experimental group were randomly assigned to three groups, thus a total of four groups entered this phase of study. The control group (Con, $n = 7$) and the model group (DHEA + HFD, $n = 9$) received 0.2 mL/10 g of distilled water by gavage. The metformin group (DHEA + HFD + Met, $n = 9$) was administered metformin hydrochloride (200 mg/kg/day) by gavage [26], while the WXZZ group (DHEA + HFD + WXZZ, $n = 8$) received a WXZZ solution (270 mg/kg/day) by gavage, calculated based on the "Equivalent Doses for Animals and Humans Based on Body Surface Area" algorithm [27], with a conversion factor of 12.3:1 for mice. The dosage for WXZZ and metformin calculate based on the body weight of mice on that day, then dissolving in 0.2 ml distilled water by gavage.

All experimental groups were maintained on HFD, while the control group received a standard diet. The treatments were administered once daily at approximately 10:00 a.m. for a duration of 2 weeks.

Assessment of estrous cycle

The estrous cycle in mice, typically lasting 4–5 days, was monitored in this study by collecting vaginal exfoliated cells daily at approximately 9:00 a.m. over 12 consecutive days. During the modeling phase, collections began on the 10th day, while in the treatment phase, collections began on the third day. Vaginal smears were obtained by flushing the vaginal canal with sterile saline, spreading the fluid onto glass slides, and fixing the samples in 4% paraformaldehyde. The smears were then stained with HE to visualize the cells [28]. Microscopic analysis of the HE-stained smears allowed for the identification of the

estrous cycle stage based on the predominant cell types (Table 1).

Measurement of FBG and other serum parameters

FPG levels were measured using an Accu-Chek Performa glucometer (Roche, Korea). To obtain the blood sample, a small incision was made at the tail tip of the mice using sterile medical scissors. A drop of blood was then applied to a test strip for glucose measurement, with results expressed in mmol/L.

For serum analysis, samples were collected from the mice's eyeballs. The collected blood was allowed to clot at 4 °C for 2 h, followed by centrifugation at 3000 rpm for 10 min to separate the serum, then the sample was stored at -80 °C until further analysis. Serum levels of T, estradiol (E_2), progesterone (P), LH, and FSH were measured using enzyme-linked immunosorbent assay (ELISA) kits (Wuhan Eliot Biotechnology Co., China). Serum NEFA levels was analyzed by a fully automated biochemical analyzer (Roche, Germany). Serum irisin (MALLBIO, MBE12290, JL21442-48 T; assay range: 2.5 ng/mL – 80 ng/mL; sensitivity: 0.1 ng/mL) and FINS (MALLBIO, MBE10122, JL10692-48 T; assay range: 1.25 mU/L – 40 mU/L; sensitivity: 0.1 mIU/L) levels were determined using double antibody one-step sandwich ELISA kits, following the manufacturer's protocols. Absorbance was measured at 450 nm using a microplate reader, and concentrations were calculated based on standard curves.

Histomorphological observations

Following the completion of blood sampling, the mice were anesthetized via intraperitoneal injection of 2% pentobarbital sodium solution (0.2 mL/100 g). Bilateral gastrocnemius muscle and abdominal adipose tissues were rapidly excised. Half of tissue specimen was used for hematoxylin-eosin (HE) staining. The remaining half was stored at -80 °C for subsequent protein and mRNA expression analyses. The tissues were processed uniformly across all groups.

Gastrocnemius muscle tissue samples were fixed in 4% paraformaldehyde for a minimum of 24 h. Following fixation, the tissues underwent gradient dehydration using a series of ethanol concentrations, followed by clearing in xylene. The cleared tissues were then embedded in paraffin wax for 4 h. Tissue sections were prepared with a thickness of 4 μm and stained sequentially with HE. The stained sections were sealed with neutral balsam and analyzed under a light microscope (Nikon, 400x magnification) for histological analysis.

Adipose tissue was stained with Oil Red O. Lipid droplet content was analyzed using an adipogenesis assay kit (cell-based: Abcam, ab133102, USA) according to the manufacturer's instructions. Briefly, cells were washed twice with Lipid Droplet Analysis Wash Solution, then Lipid Droplet Analysis Oil Red O solution was added to the cells, and the cells were incubated at room temperature for 20 min before staining was observed microscopically. Stained lipid droplets were detected by reading the absorbance at 490 nm using enzyme standards.

Table 2 Details of the antibodies used in Western blotting

Antibody	Company	Cat. no.	Dilution
AMPK	CST	#2532	1:1000
PGC1-α	Abcam	ab191838	1:1000
FNDC5	Abcam	ab174833	1:1000
Irisin	Abcam	ab181389	1:1000
CaMKK	CST	#16,810	1:1000
UCP1	CST	#14,670	1:1000
GAPDH	Abcam	ab9485	1:2500
Anti-rabbit IgG (HRP)	Beyotime	A0208	1:1000

Western blot analysis

Western blotting was employed to detect the protein levels of AMPK, PGC-1α, FNDC5, and irisin in the gastrocnemius muscle tissues and CaMKK, AMPK, PGC1-α, and UCP1 in subcutaneous fatty tissue [29]. Proteins were extracted from the target tissues by homogenizing the samples in RIPA Tissue Cell Rapid Lysis Solution (R0020, Beijing Solepol) containing protease inhibitors. The homogenates were lysed thoroughly, and the supernatant was collected following centrifugation. The protein concentration of the extracted samples was measured using the BCA Protein Assay Kit (PICPI23223, Thermo Fisher Scientific). The extracted proteins were separated by SDS-PAGE (S1010, Beijing Solepol) and subsequently transferred onto nitrocellulose (NC) membranes (HATF00010, Millipore) through electroblotting. The membranes were blocked overnight at 4 °C in a 5% skim milk powder (D8340, Solepol, Beijing) blocking solution to prevent non-specific binding.

Immunoblotting was performed by incubating the membranes with primary antibodies against AMPK, PGC1-α, FNDC5, irisin, CaMKK, UCP1 (Table 2) for 24 h at 4 °C. After incubation, the membranes were washed and then incubated with the corresponding secondary antibodies. Glyceraldehyde-3-phosphate dehydrogenase (GAPDH) was used as a loading control. Enhanced chemiluminescence signals were detected using a chemiluminescence imaging system (chemq3400mini, China), and the gray values of the protein bands were quantitatively analyzed using ImageJ software. The process was repeated at least three times to ensure reproducibility and reliability of the results.

RT-PCR assay

Reverse transcription-polymerase chain reaction (RT-PCR) was utilized to quantify mRNA expression of AMPK, PGC1-α, FNDC5, and irisin in gastrocnemius

muscle tissues and CaMKK, AMPK, PGC1-α, annd UCP1 in subcutaneous fatty tissue [30]. Total RNA was extracted from tissue samples using TRIzol reagent (1596-026, Invitrogen, USA). To remove genomic DNA, RNA was treated with DNase I according to the instructions provided with the reverse transcription kit (Fermentas, #K1622, USA). Complementary DNA (cDNA) was synthesized from the purified RNA. cDNA was amplified using the SYBR Green PCR kit (#K0223, Thermo Fisher Scientific) and analyzed with a Real-Time PCR detector (ABI-7300, ABI Corp.). The PCR conditions were set as follows: denaturation at 95 °C for 15 s, annealing at 55 °C for 45 s, and extension at 72 °C for 30 s, for a total of 40 cycles. The relative expression levels were calculated using the $2^{-\Delta\Delta Ct}$ method, with GAPDH serving as the internal control for normalization. The specific primers used are detailed in Table 3.

Statistical analysis

Statistical analyses were conducted using SPSS version 26.0 and GraphPad Prism version 9.0.0. All data are presented as mean ± standard deviation (SD) and were validated for normal distribution using the shapiro-wilk test before subsequent statistical analyses. Intergroup differences were compared using the student's t-test for two groups and one-way ANOVA for three or more groups.

Table 3 Primer sequence used for RT-PCR

Gene	Primer	Sequence	Size(bp)	GeneBank ACC
AMPK	Forward	5′AAACCCACAG AAATCCAAAC 3′	114	NM_001013367.3
	Reverse	5′TGCTTGATTGC TCTACAAAC 3′		
PGC1-α	Forward	5′TGGATTGAAGT GGTGTAG 3′	180	NM_001402987.1
	Reverse	5′GTCAGTGCATC AAATGAG 3′		
FNDC5	Forward	5′CATTGTTGTGG TCCTCTTC 3′	222	NM_027402.4
	Reverse	5′CGCATTCTCTA CTGTCTTC 3′		
Irisin	Forward	5′GAGCCCAATA ACAACAAG 3′	236	NM_006503212.5
	Reverse	5′AATAAGCCCG ATGATAGG 3′		
CaMKK	Forward	5′GTCCACAGGG ACATCAAG 3′	203	NM_001362841.1
	Reverse	5′GTGGCCCATAC ATCCAAG 3′		
UCP1	Forward	5′CATTCAGAGG CAAATCAG 3′	135	NM_009463.3
	Reverse	5′ACACCTCCAG TCATTAAG 3′		
GAPDH	Forward	5′ATCACTGCCAC CCAGAAG 3′	191	NM_008084.2
	Reverse	5′TCCACGACGG ACACATTG 3′		

For non-normally distributed data, the kruskal-wallis test was employed. Correlation analyses were performed using Pearson's correlation coefficient or normally distributed variables and Spearman's correlation coefficient for non-normally distributed variables. $P < 0.05$ was considered as statistically significant.

Results

Component of the WXZZ decoction

The WXZZ decoction contained Atractylodes macrocephala 30 g (Baizhu), Astragalus membranaceus 15 g (Huangqi), Citrus reticulata 15 g (Chenpi), Codonopsis pilosula 15 g (Dangshen), Cimicifuga foetida 10 g (Shengma), Bupleurum chinense 10 g (Chaihu), Angelica sinensis 9 g (Danggui), Glycyrrhiza uralensis 6 g (Gancao), Poria cocos 10 g (Fuling), Taxillus chinensis 15 g (Sangjisheng), Cyperus rotundus 10 g (Xiangfu), Achyranthes bidentata 10 g (Niuxi), Lycium barbarum 10 g (Gouqizi), Morinda officinalis 10 g (Bajitian), Pueraria lobata 15 g (Gegen).

Establishment of IR and anovulatory mice model

We successfully established IR and anovulatory mice model. Representative images of vaginal cytology at each estrous stage are shown in Fig. 1A. Our study found that compared with the control group, the mice in DHEA + HFD group had prolonged intervals between estrous cycles or were in a state of stagnation (mainly dominated by the estrous and menopausal phases), and the distribution of the cycles was significantly unbalanced (Fig. 1B, C). The weight in DHEA + HFD group increased faster than that of in control group (Fig. 1D). After 21 days of continuous induction of DHEA and HFD, as compared with control group, mice in DHEA + HFD group exhibited significant elevation of body weight, FINS and HOMA-IR, elevation of serum T, LH and LH/FSH ratio (Fig. 1E-J). These results indicate that our study successfully constructed mice model of PCOS combined with IR (i.e., HA and ovarian anovulatory type). In addition, serum E_2 was elevated and P was reduced in DHEA + HFD group compared to the control group, whereas there is no statistical discrepancy in FPG and FSH levels between the two groups (Supplementary Fig. 1).

WXZZ ameliorates endocrine-metabolic disorders and restores menstrual cycle in IR and anovulatory mice

After 2 weeks of consecutive gavage treatment, compared with the control group, the DHEA + HFD group had an irregular motility cycle and an unbalanced distribution of the proportion of each period. However, compared to the DHEA + HFD group, the estrous cycles of the DHEA + HFD + Met and DHEA + HFD + Wxzz groups were progressively more regular, with a relatively

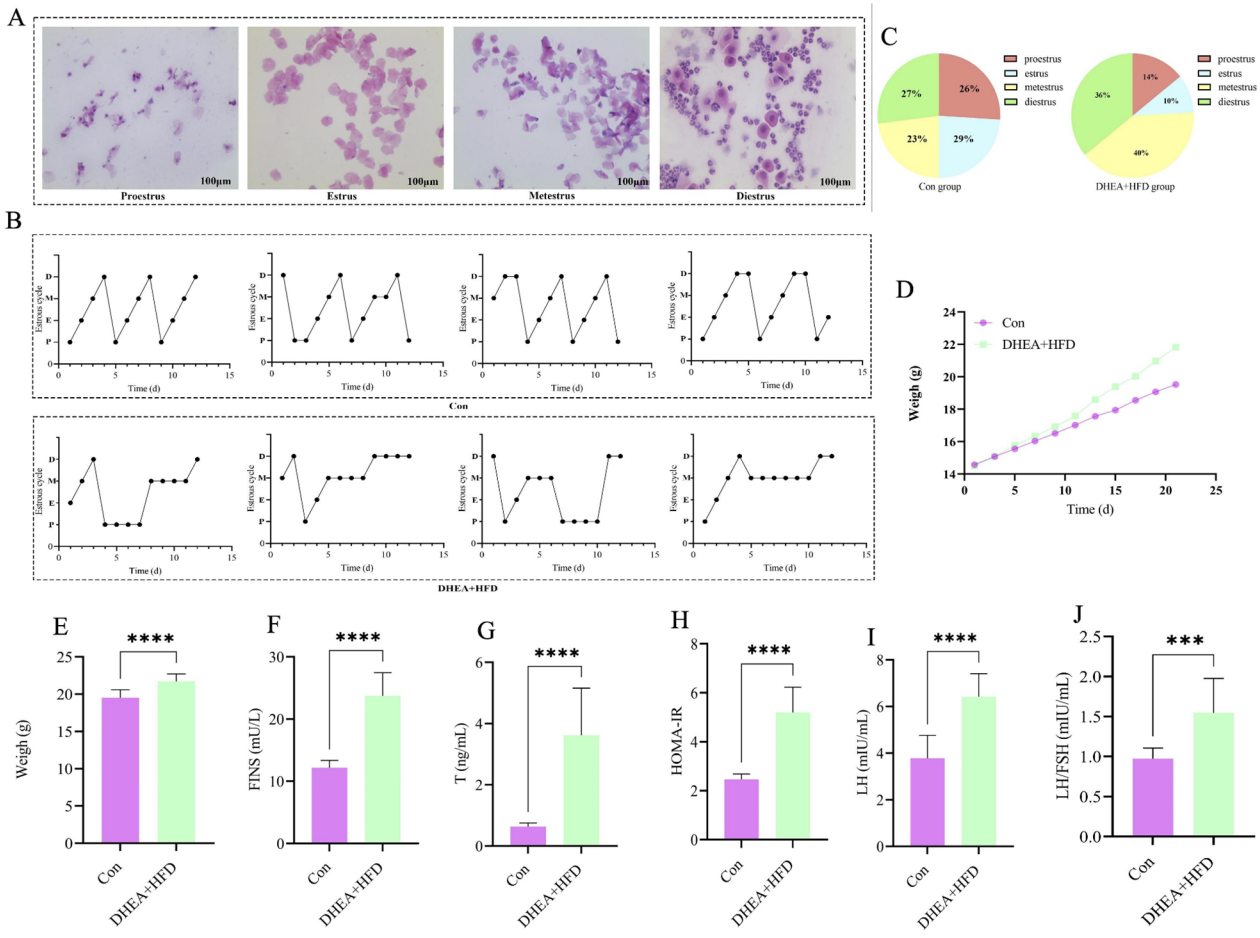

Fig. 1 DHEA subcutaneous injection combined with HFD feeding induces the mice with PCOS combined with IR. For **A-D**, the mice were divided into two groups (Control, DHEA + HFD). For **A-C**, DHEA subcutaneous injection combined with HFD feeding significantly disrupted the estrous cycle of mice. (**A**) The estrous cycle of mice ($n = 10$ mice per group) was observed for 12 days. P: Proestrus, E: Estrus, M: Metestrus, D: Diestrus. (**B**) **H**&**E**stained smears of vaginal secretions at four stages of the estrous cycle in mice (magnification 100×). (**C**) Proportion of estrous cycle stages in mice. (**D**) Body Weight, FINS, HOMA-IR, Testosterone, E_2, P, LH, LH/FSH ($n = 8$ mice per group). Data were analyzed by unpaired samples t-test and are expressed as mean ± SEM. $^{*}P < 0.05$. $^{**}P < 0.001$. $^{***}P < 0.0001$

balanced proportion of each cycle (Fig. 2A, B). Weight gain was faster in the DHEA + HFD group compared to the control group, and the Met and Wxzz interventions slowed this elevated trend, respectively (Fig. 2C). Body weight, FINS, HOMA-IR, T, LH and LH/FSH were significantly higher in the DHEA + HFD group compared to the control group. However, the DHEA + HFD + Met and DHEA + HFD + Wxzz groups showed significant decreases in body weight, FINS, and HOMA-IR, and decreases in serum T, LH, and LH/FSH compared to the DHEA + HFD group (Fig. 2D-I). Wxzz had slightly better weight loss than Met, but there was no statistical difference. Interestingly after Wxzz interventions, our study did not find differences in FBG, E2, P, and FSH among 4 groups (Supplementary Fig. 2).

WXZZ promotes irisin secretion

To investigate whether WXZZ exerts beneficial effect on mice with PCOS-combined IR by affecting irisin secretion, we examined irisin level in 24 mice (6 mice randomized in each group). Serum irisin level was significantly lower in the DHEA + HFD group compared to the control group. Whereas, it was significantly higher in the DHEA + HFD + Met and DHEA + HFD + Wxzz groups compared with the DHEA + HFD group (Fig. 3A). Pearson correlation analysis showed a negative correlation between irisin and body weight, FINS, HOMA-IR, T, LH, and LH/FSH (Fig. 3B). These data suggest that Wxzz treatment may ameliorate metabolic and endocrine disorders in mice with PCOS combined with IR by promoting irisin secretion.

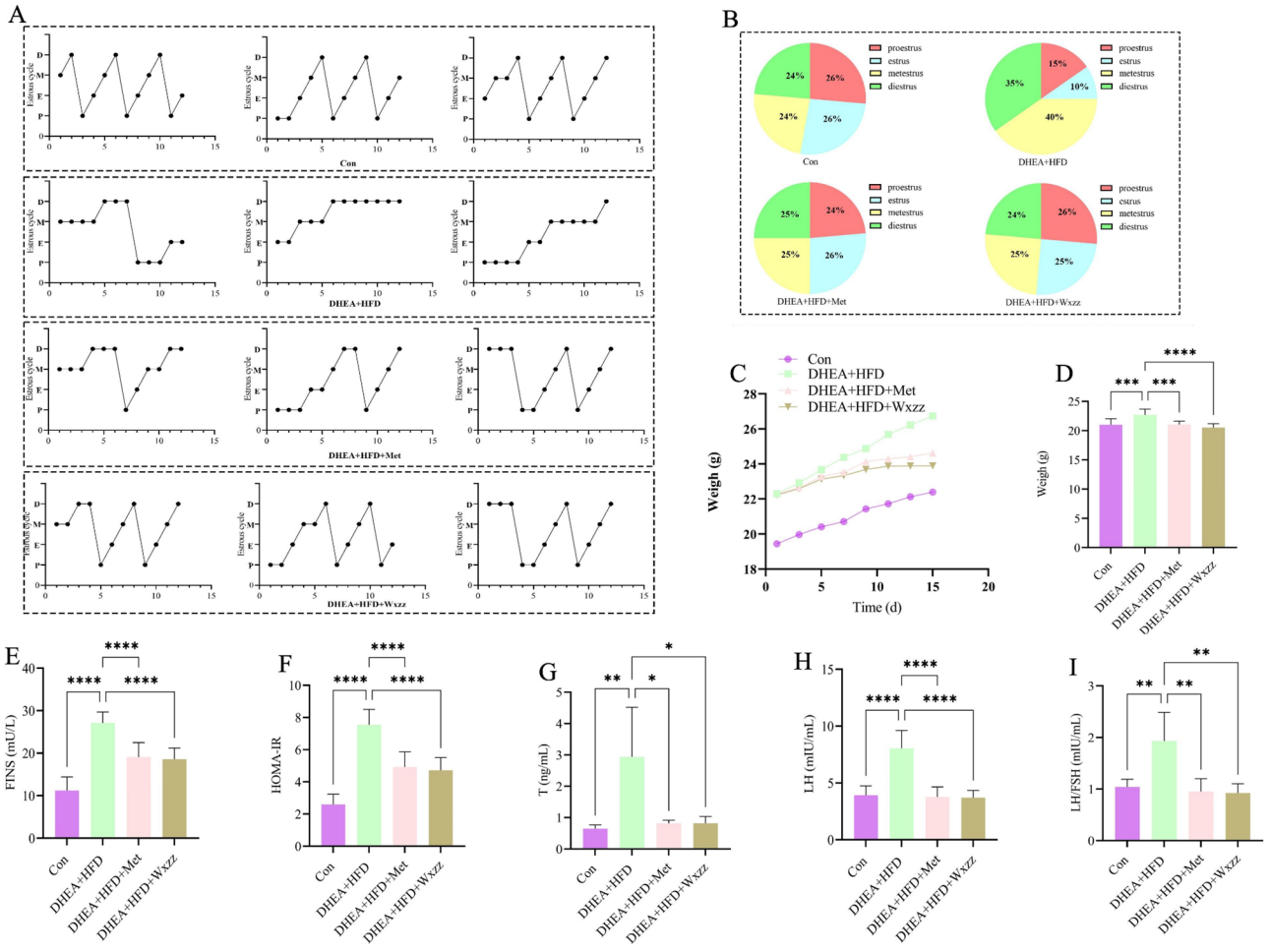

Fig. 2 Wxzz treatment improved the estrous cycle, insulin and hormone level disorder of mice with PCOS and IR induced by DHEA and HFD. For **A-C**, the mice were divided into four groups (control, DHEA + HFD, DHEA + HFD + Met, DHEA + HFD + Wxzz). For **A-C**: Wxzz treatment significantly improved the estrous cycle disorder of the mice. (**A**) The estrous cycle of mice ($n = 6$ mice per group) was observed for 12 days. P: Proestrus, E: Estrus, M: Metestrus, D: Diestrus. (**B**) Proportion of estrous cycle stages in mice. (**D**) Body Weight, FINS, HOMA-IR, Testosterone, LH, LH/FSH ($n = 6$ mice per group). Data were analyzed using one-way ANOVA with Tukey's multiple comparison post-hoc test and data are presented as means ± SEM. $^{*}P < 0.05$. $^{**}P < 0.001$. $^{***}P < 0.0001$

WXZZ partially reverses the structure of the gastrocnemius muscle

In the control group, gastrocnemius muscle cells were neatly aligned, polygonal in shape, with well-defined borders, and nuclei positioned close to the cell periphery, maintaining regular shape and size. In contrast, the DHEA + HFD group exhibited disorganized muscle fibers, with cells appearing rounded, deformed, and fragmented. There was an increase in the extracellular space, and cell nuclei tended to cluster toward the center of the cells. Compared to the DHEA + HFD group, the DHEA + HFD + Met and DHEA + HFD + WXZZ groups showed partial restoration of structure of the gastrocnemius muscle (Fig. 4A).

WXZZ upregulates AMPK/PGC1-α/FNDC5/Irisin protein and mRNA expression in gastrocnemius muscle

We found that the protein and mRNA expression levels of AMPK, PGC1-α, FNDC5, and irisin were significantly lower in the DHEA + HFD group compared to the control group, which indicated that the expression of irisin pathway-related molecules in the gastrocnemius muscle were downregulated. In the DHEA + HFD + WXZZ group, the expression of these molecules was significantly elevated compared to the DHEA + HFD and DHEA + HFD + Met group (Fig. 4B-J), which may explain the superior therapeutic effects of WXZZ.

WXZZ inhibits NEFA secretion

We found that serum NEFA levels were significantly higher in the DHEA + HFD group compared to the control group. Whereas, the NEFA were significantly lower in both DHEA + HFD + Met and DHEA + HFD + Wxzz

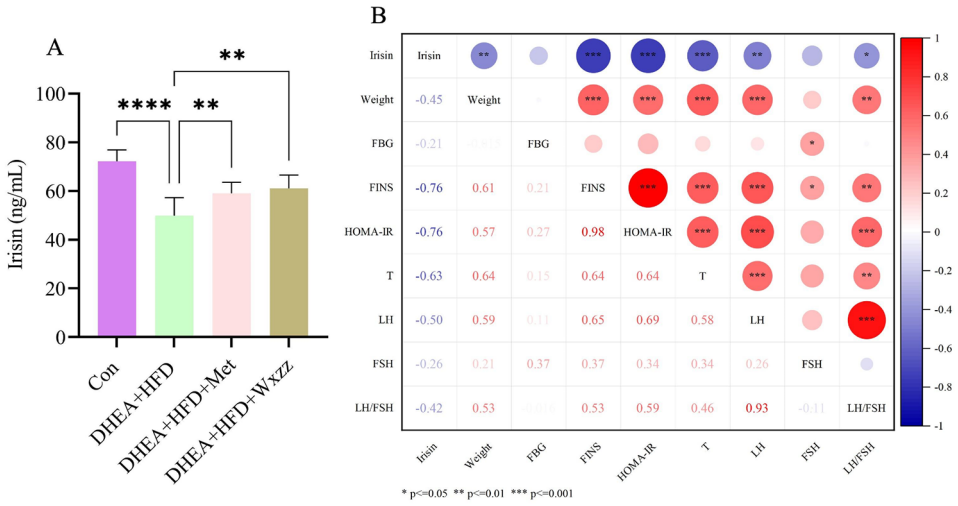

Fig. 3 Wxzz increased serum irisin levels in DHEA and HFD-induced PCOS combined IR mice. Serum irisin levels were significantly negatively correlated with body weight, FINS, HOMA-IR, T, LH, and negatively correlated with LH/FSH. (**A**) Quantitative analysis of serum irisin levels in mice ($n=6$ mice per group). Data were analyzed by one-way ANOVA and Tukey's multiple comparisons post hoc test and are expressed as mean ± SEM. (**B**) Correlation analysis of irisin with body weight, metabolism, and hormone levels ($n=6$ mice per group). Data were analyzed using Pearson's correlation analysis. $^{*}P<0.05$. $^{**}P<0.001$. $^{***}P<0.0001$

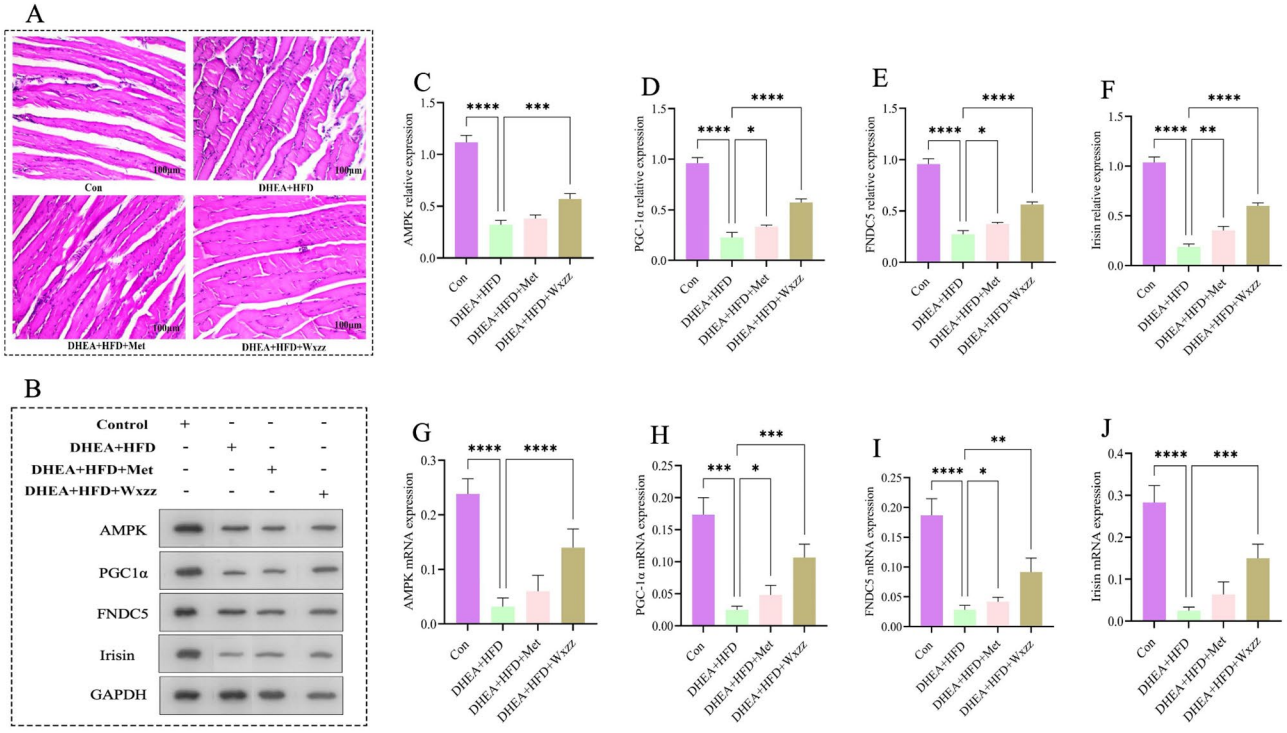

Fig. 4 Wxzz ameliorates pathological changes in gastrocnemius muscle structure in DHEA and HFD-induced PCOS combined with IR mice. Wxzz promotes protein and gene expression of AMPK, PGC1-α, FNDC5, and Irisin in gastrocnemius muscle of mice. (**A**) Representative H&E staining plots of gastrocnemius muscle (6 mice per group). Scale bar: 10 μm (magnification: 10×10). (**B**) Protein expression levels of AMPK, PGC1-α, FNDC5, Irisin in gastrocnemius muscle tissues. (**C**) Protein quantification with AMPK, PGC1-α, FNDC5, Irisin. Relative mRNA levels of AMPK, PGC1-α, FNDC5, Irisin genes in gastrocnemius muscle tissues. Data were analyzed by one-way ANOVA and Tukey's multiple comparisons post hoc test and are expressed as mean ± SEM. $^{*}P<0.05$. $^{**}P<0.001$. $^{***}P<0.0001$

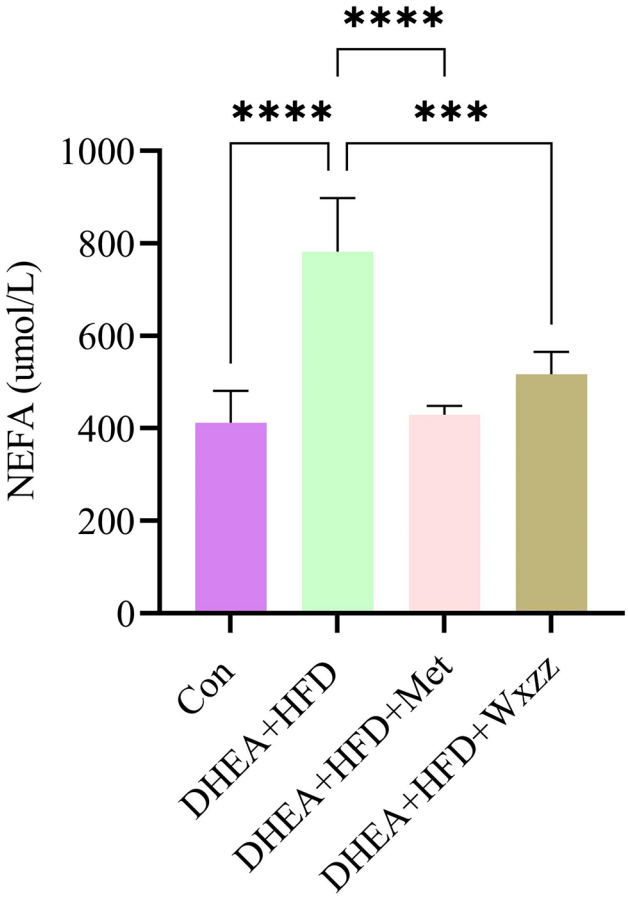

Fig. 5 Wxzz reduces serum NEFA levels in DHEA and HFD-induced PCOS combined IR mice. Quantitative analysis of serum NEFA levels in mice ($n = 6$ mice per group). Data were analyzed by one-way ANOVA and Tukey's multiple comparisons post hoc test and are expressed as mean ± SEM. $^{*}P < 0.05$. $^{**}P < 0.001$. $^{***}P < 0.0001$

groups compared to the DHEA + HFD group (Fig. 5). Interestingly Met inhibited NEFA overproduction more significantly compared to Wxzz.

WXZZ partially reverses the structure of the abdominal adipose

We found that the adipose tissue in the DHEA + HFD group presented a greater number and area of lipid droplets compared to the Con group. Compared to the DHEA + HFD group, the number and volume of lipid droplets were significantly reduced in the DHEA + HFD + Met and DHEA + HFD + Wxzz groups. This suggests that Met and Wxzz can partially reverse the damaged adipose tissue in the pathological setting of IR and anovulatory mice, respectively, and mobilize the adipose tissue to increase energy expenditure, reduce lipid production, and ameliorate fat accumulation (Fig. 6A).

WXZZ upregulates CaMKK/AMPK/PGC1-α/UCP1 protein and mRNA expression in abdominal adipose

We found that the protein and mRNA expression of CaMKK, AMPK, PGC1-α and UCP1 were significantly lower in the DHEA + HFD group compared to the Con group. Whereas, protein and mRNA expression of all these molecules was significantly higher in the DHEA + HFD + Wxzz group compared to the DHEA + HFD group (Fig. 6B-J). It suggests that IR and anovulatory pathological environment decreased the expression of AMPK/PGC1-α pathway-related molecules in adipose tissues, while Wxzz might promote WAT browning, mediate calorie production, and increase energy expenditure by modulating the expression of these cellular energy metabolism-related molecules. UCP1 plays an important role in mitochondrial biogenesis, which may be a reason for the beneficial effects of Wxzz on adipose tissue in PCOS combined with IR mice.

Discussion

In this study, we successfully established mice model of IR and anovulatory and demonstrated that treatment with WXZZ had significant therapeutic effects. WXZZ not only restored the estrous cycle but also effectively reduced body weight, serum T, LH, the LH/FSH ratio, FINS, and HOMA-IR, thereby improving the overall PCOS-IR status. Importantly, our findings indicate that WXZZ treatment led to a significant increase in serum irisin levels, reduced NEFA levels and partial restoration of the gastrocnemius muscle and subcutaneous adipose structure. Furthermore, WXZZ significantly upregulated the protein and mRNA expression levels of AMPK, PGC1-α, FNDC5, and irisin in the gastrocnemius muscle tissues and CaMKK, AMPK, PGC1-α, and UCP1 in subcutaneous adipose tissue. These molecular changes suggest that the therapeutic effects of WXZZ in the IR and anovulatory mice model may be mediated through the regulation of the AMPK/PGC-1α/irisin pathway.

Metformin is widely recommended as a first-line therapeutic agent for type 2 diabetes due to its well-established effects on IR and hormonal regulation [31]. Its therapeutic applications have also extended into the field of reproductive health, particularly in the treatment of PCOS, where it has been shown to improve metabolic disturbances in patients with PCOS-IR [32]. Additionally, studies have suggested that metformin may promote cell proliferation and inhibit apoptosis by upregulating irisin expression via activation of the AMPK/SIRT1/PGC1-α signaling pathway [33]. Given these properties, metformin was used as a comparator in our study. We found that WXZZ not only exhibited similar effects to metformin but also demonstrated superior efficacy in regulating the AMPK/PGC1-α/irisin pathway in mice with PCOS-IR.

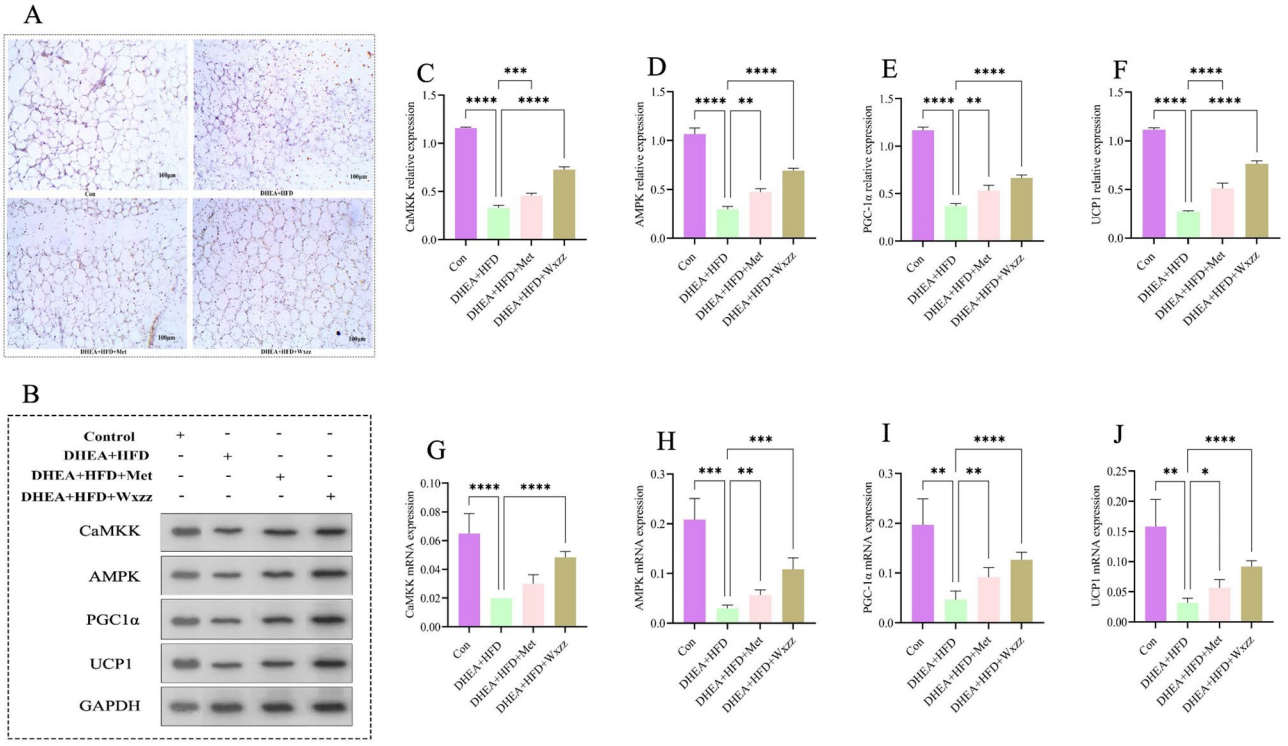

Fig. 6 Wxzz ameliorates pathological changes in abdominal adipose structure in DHEA and HFD-induced PCOS combined with IR mice. Wxzz promotes protein and gene expression of CaMKK, AMPK, PGC1-α, and UCP1 in abdominal adipose of mice. (**A**) Representative oil red O staining plots of adipose tissue (6 mice per group). Scale bar: 10 μm (magnification: 10 × 10). (**B**) Protein expression levels of CaMKK, AMPK, PGC1-α, UCP1 in adipose tissue. (**C**) Protein quantification with CaMKK, AMPK, PGC1-α, UCP1. Relative mRNA levels of CaMKK, AMPK, PGC1-α, UCP1 genes in adipose tissue. Data were analyzed by one-way ANOVA and Tukey's multiple comparisons post hoc test and are expressed as mean ± SEM. *$P < 0.05$. **$P < 0.001$. ***$P < 0.0001$

Previous studies have indicated that serum irisin levels are reduced in several metabolic disorders, including obesity, type 2 diabetes, and PCOS [34–36]. For instance, a study involving 49 women with PCOS and 39 BMI- and age-matched healthy controls found that serum irisin concentrations were significantly lower in women with PCOS compared to the control group. Additionally, this study observed a negative correlation between serum irisin and LH levels [37]. Another study presented a different perspective, suggesting that irisin levels are actually elevated in patients with PCOS, particularly in those with IR, compared to healthy controls [38]. Our study demonstrates that serum irisin is significantly lower in PCOS-IR mice compared to the health mice. This is a supplement to the research on irisin and PCOS-IR, and is also the basis for further research. The discrepancy may be attributed to a compensatory protective mechanism in PCOS patients [39], wherein elevated irisin levels potentially play a role in preventing the progression of PCOS-related complications by enhancing metabolic activity, increasing energy expenditure, reducing body mass, and counteracting the effects of hyperinsulinemia and other metabolic disruptions associated with decreased insulin sensitivity [40, 41]. However, studies on irisin and obesity, IR, and polycystic ovary syndrome are inconsistent. Irisin is negatively correlated with HOMA-IR in healthy people and positively correlated with PCOS patients [42]. There are few studies on serum levels of irisin in patients with PCOS combined with IR. Irisin in women with normal androgenic PCOS were similar to healthy women and lower than those of other phenotypes [43]. In addition, irisin levels were higher [43], lower [37] in patients with PCOS than in controls. Therefore, the results of irisin and PCOS are controversial. Irisin and insulin levels are negatively correlated [44], whereas other studies have found a positive correlation [34]. These differences may be related to significant heterogeneity in published studies. Furthermore, it is important to consider confounding factors such as BMI, insulin sensitivity, different phenotypes, the precision of measurement instruments, and the timing of interventions, all of which could contribute to the observed differences in irisin levels across studies.

Irisin, an identified exercise-induced myokine, has also been shown to enhance muscular fitness through the activation of the AMPK/PGC1-α/irisin pathway, particularly in response to chronic physical exercise [45]. Physical exercise is widely recommended for patients with PCOS, as it not only helps lose weight, but help restore ovulation and alleviate numerous PCOS symptoms and [46]. The findings of our study suggest that WXZZ may

exert effects like those of physical exercise, potentially offering therapeutic benefits for patients with PCOS.

NEFA is an intermediate product of lipid metabolism. When NEFA increases beyond the storage capacity of fat, it causes lipid accumulation and tissue damage. Dysfunction of WAT and BAT in the pathologic setting of PCOS causes excessive release of NEFA and affects secretion of adipokines and cytokines [47]. In obese PCOS patients, lipolysis is more pronounced than lipogenesis due to reduced resistance to the anti-adipolytic effects of insulin, resulting in NEFA overload [48]. The excess NEFA further leads to ectopic deposition of fat in other tissues, causing BAT dysfunction. However, there have negative [49], positive [50] and no significant correlation between BMI and irisin [37].

We identified two studies [51, 52] that explored the use of an herbal formulation for treating PCOS, which included several herbs also found in our formulation, such as Xiangfu, Chenpi, and Huangqi. These herbs are traditionally associated with regulating "Qi function," suggesting that Qi dysfunction might be a crucial factor in the pathogenesis of PCOS. According to traditional Chinese medicine theory, Qi plays a vital role in regulating the flow of blood, fluids, and liquids throughout the body [17]. When Qi is unable to facilitate their movement effectively, these substances can become stagnant, leading to the formation of phlegm, water-dampness, and blood stasis, which can contribute to the development of serious health issues [18]. Thus, addressing Qi dysfunction is an important therapeutic strategy in managing PCOS [53].

There are several limitations in our study. The major finding of this study highlights WXZZ as a promising therapeutic strategy against DHEAS and high-fat diet-induced IR and anovulatory mice, acting through the AMPK/PGC-1α/irisin pathway. In addition, our study is temporarily unable to provide morphological observations and protein and gene expression levels of ovarian tissue. Future studies to investigate other possible mechanisms for the beneficial effects of WXZZ would provide more comprehensive understanding. Such as the browning of WAT. Given that the thermogenesis of brown adipose tissue (BAT) is negatively correlated with androgen levels, increasing BAT activity could be particularly beneficial for patients with PCOS [54, 55]. Besides, due to technical limitations, we investigated the effects of WXZZ primarily using DHEAS and high-fat diet-induced IR and anovulatory mice model. It does not fully replicate the complexity of the condition in human patients. Induction instability of the IR and anovulatory mice model may occur using aged mice. Subsequent studies can be analyzed based on the age of the mice, making the conclusions more reliable. Therefore, while our findings suggest that the AMPK/PGC1-α/irisin pathway may play a role in IR and anovulatory mice, further studies are needed to confirm its relevance in clinical settings. Finally, we did not analyze the chemical components of the WXZZ decoction, future research should include a detailed chemical characterization of WXZZ to better understand the specific compounds responsible for its therapeutic effects.

Conclusion

We demonstrate that the Chinese herbal formulation WXZZ has therapeutic effects in restoring estrous cycle and improving insulin sensitivity in DHEAS and high-fat diet-induced IR and anovulatory mice, as well as in reversing the structural damage of the gastrocnemius muscle and subcutaneous fat. Treatment with WXZZ led to an increase in serum irisin levels, accompanied by enhanced expression of AMPK/PGC1-α/FNDC5/irisin proteins and mRNA in gastrocnemius and CaMKK/AMPK/PGC1-α/UCP1 proteins and mRNA in adipose tissues. In conclusion, our study has suggested that WXZZ may improve the endocrine and metabolic disorders of the IR and anovulatory by promoting the secretion of irisin and increasing energy expenditure.

Abbreviations

PCOS	Polycystic ovary syndrome
IR	Insulin resistance
TCM	Traditional Chinese Medicine
Wxzz	Woxuanzhongzhou
Met	Metformin
DHEA	Dehydroepiandrosterone
HFD	High-fat diet
AMPK	Adenosine 5'-monophosphate (AMP)-activated protein kinase
PGC1-α	Peroxisome proliferator-activated receptor-γ coactivator 1α
FNDC5	Recombinant fibronectin type III domain containing protein 5
CaMKK	Calmodulin-dependent protein kinase kinase
UCP1	Uncoupling protein 1
BMI	Body mass index
HA	Hyperandrogenemia
WAT	White adipose tissue
BAT	Brown adipose tissue
WHR	Waist-to-hip ratio
AEC	Animal experiment center
BUCM	Beijing university of chinese medicine
FBG	Fasting blood glucose
FINS	Fasting insulin
T	Testosterone
P	Progesterone
E_2	Estradiol
LH	Luteinizing hormone
FSH	Follicle stimulating hormone
AMH	Anti-mullerian hormone
HE	Hematoxylin-eosin
NEFA	Nonesterified fatty acid
GAPDH	Glyceraldehyde-3 phosphate dehydrogenase

Supplementary Information

The online version contains supplementary material available at https://doi.org/10.1186/s13048-025-01587-5.

Supplementary Material 1

Supplementary Material 2

Supplementary Material 3

Acknowledgements
We thanks all the reviewers for their helpful suggestions and comments about our study.

Author contributions
Haijuan Liu designed the study, analyzed and interpreted the experimental data, and was a major contributor to writing the manuscript. Guohua Wang and Conglu Sui performed histological examination of the specimens. Yanan Guo wrote part of the manuscript. Xiangyu He completed the experiments. All authors read and approved the final manuscript.

Funding
This work was supported by the Beijing University of Chinese Medicine Key Discipline Construction Program Fund (grant number 90010951310079); Beijing University of Chinese Medicine Vertical Development Fund for University-level Research (grant number 2023-SFYZX-09); The Third Affiliated Hospital of Beijing University of Chinese Medicine 2022 Institutional Cultivation Programs (grant numbers BZYSY-2022-PYMS-13); Basic Research Program of Beijing University of Chinese Medicine (grant number 2018-JYBZZ-JS138).

Data availability
No datasets were generated or analysed during the current study.

Declarations

Ethical approval
All animal experimental procedures were agreed and approved by the Laboratory Animal Ethics Sub-committee of the Academic Committee of Beijing University of Chinese Medicine (BUCM) (No.: BUCM-2023030104-1105).

Consent for publication
Not applicable.

Competing interests
The authors declare no competing interests.

Author details
[1]Department of Gynecology, Third Affiliated Hospital of Beijing University of Chinese Medicine, Beijing 100029, China
[2]Department of Traditional Chinese Medicine, Northwest Women's and Children's Hospital, Xi'an 710061, China
[3]Shunyi Hospital, Beijing Traditional Chinese Medicine Hospital, Beijing 101300, China

Received: 11 August 2024 / Accepted: 3 January 2025
Published online: 16 January 2025

References

1. Azziz R, et al. Polycystic ovary syndrome. Nat Rev Dis Primers. 2016;2:16057.
2. Li L, et al. Association between mild depressive states in polycystic ovary syndrome and an unhealthy lifestyle. Front Public Health. 2024;12(12):1361962.
3. Chen T et al. The relationship between polycystic ovary syndrome and insulin resistance from 1983 to 2022: A bibliometric analysis. Front Public Health. 2022;10:960965. https://doi.org/10.3389/fpubh.2022.960965.
4. Amisi CA. Markers of insulin resistance in polycystic ovary syndrome women: an update. World J Diabetes. 2022;13(3):129–49.
5. Luo Y, et al. Irisin: circulating levels in serum and its relation to gonadal axis. Endocrine. 2022;75(3):663–71.
6. Lin J, et al. Exercise ameliorates muscular excessive mitochondrial fission, insulin resistance and inflammation in diabetic rats via irisin/AMPK activation. Sci Rep. 2024;14(1):10658.
7. Aydin S, et al. A comprehensive immunohistochemical examination of the distribution of the fat-burning protein irisin in biological tissues. Peptides. 2014;61:130–6.
8. Li H, et al. Free androgen index and irisin in polycystic ovary syndrome. J Endocrinol Investig. 2015;39(5):549–56.
9. Zhang L, et al. The association between circulating irisin levels and different phenotypes of polycystic ovary syndrome. J Endocrinol Investig. 2018;41(12):1401–7.
10. Chang CL, et al. The serum level of irisin, but not asprosin, is abnormal in polycystic ovary syndrome patients. Sci Rep. 2019;9(1):6447.
11. Boström P, et al. A PGC1-α-dependent myokine that drives brown-fat-like development of white fat and thermogenesis. Nature. 2012;481(7382):463–8.
12. Yang Y et al. Dihydromyricetin ameliorates hepatic steatosis and insulin resistance via AMPK/PGC-1α and PPARα-mediated autophagy pathway. J Translational Med, 2024. 22(1).
13. Kim H, et al. Irisin mediates effects on Bone and Fat via αV Integrin receptors. Cell. 2018;175(7):1756–e176817.
14. Toyama EQ, et al. AMP-activated protein kinase mediates mitochondrial fission in response to energy stress. Science. 2016;351(6270):275–81.
15. Arhire LI, Mihalache L, Covasa M. Irisin: a hope in understanding and managing obesity and metabolic syndrome. Front Endocrinol. 2019;10(2):00524.
16. Eisenhardt S, Fleckenstein J. Traditional Chinese medicine valuably augments therapeutic options in the treatment of climacteric syndrome. Arch Gynecol Obstet. 2016;294(1):193–200.
17. Wang Q. Ontology of Qi in Traditional Chinese Medicine based on China Philosophy and Modern Science. J Beijing Univ Chin Med. 2022;45(1):1–10.
18. Huang Y, et al. Progress in Traditional Chinese Medicine for the treatment of Migraine. Am J Chin Med. 2020;48(08):1731–48.
19. Li S, Xutian S. New Development in Traditional Chinese Medicine: symbolism-digit therapy as a special naturopathic treatment. Am J Chin Med. 2016;44(07):1311–23.
20. Chen X, Wang X. Effect of Ziyin and Qianyang Method of Traditional Chinese Medicine on PI 3K/Akt Signal Pathway, sex hormone and insulin related indexes in rats with polycystic ovary syndrome and insulin resistance. J Tradit Chin Med. 2024;42(2):23–8.
21. Shao C, Dong W, Zhang H. Application of Guijiaosan Shenque acupoint paste can improve the scores of obesity, endocrine and TCM symptoms in treating obese polycystic ovary syndrome. Am J Transl Res. 2021;13(9):10694–702.
22. Qian L, et al. Peroxisome proliferator-activated receptor gamma coactivator-1 (PGC-1) family in physiological and pathophysiological process and diseases. Signal Transduct Target Ther. 2024;9(1):50.
23. Weng Y, et al. Exercise-induced irisin improves follicular dysfunction by inhibiting IRE1α-TXNIP/ROS-NLRP3 pathway in PCOS. J Ovarian Res. 2023;16(1):151.
24. Wang X, et al. Effects of dehydroepiandrosterone alone or in combination with a high-fat diet and antibiotic cocktail on the heterogeneous phenotypes of PCOS mouse models by regulating gut microbiota. Front Endocrinol. 2022;13(12):1030151.
25. Abdi A, et al. The effect of adipose-derived mesenchymal stem cell transplantation on ovarian mitochondrial dysfunction in letrozole-induced polycystic ovary syndrome in rats: the role of PI3K-AKT signaling pathway. J Ovarian Res. 2024;17(1):91.
26. Peng Q, et al. Metformin improves polycystic ovary syndrome in mice by inhibiting ovarian ferroptosis. Front Endocrinol. 2023;14(1):1070264.
27. Nair A, Jacob S. A simple practice guide for dose conversion between animals and human. J Basic Clin Pharm. 2016;7(2):27–31.
28. Ajayi AF, Akhigbe RE. Staging of the estrous cycle and induction of estrus in experimental rodents: an update. Fertility Res Pract. 2020;6(1):65.
29. Lee JS, et al. Influence of irradiation on capsules of silicone implants covered with Acellular dermal matrix in mice. Aesthetic Plast Surg. 2021;46(2):937–46.
30. Cheng X, Li Y, Wang H. Activation of Wnt/β-catenin signal induces DCs to differentiate into immune tolerant regDCs in septic mice. Mol Immunol. 2024;172:38–46.
31. Davies MJ, et al. Management of hyperglycaemia in type 2 diabetes, 2022. A consensus report by the American Diabetes Association (ADA) and the European Association for the Study of Diabetes (EASD). Diabetologia. 2022;65(12):1925–66.
32. El Leithy AA, et al. Spirulina versus metformin for controlling some insulin signaling pathway genes in induced polycystic ovary syndrome rat model. Gene. 2024;921(30):148524.
33. Li Q, et al. Metformin-induced autophagy and irisin improves INS-1 cell function and survival in high-glucose environment via AMPK/SIRT1/PGC-1α signal pathway. Volume 7. Food Science & Nutrition; 2019. pp. 1695–703. 5.
34. Wang W, et al. Abnormal irisin level in serum and endometrium is associated with metabolic dysfunction in polycystic ovary syndrome patients. Clin Endocrinol. 2018;89(4):474–80.

35. Yang X, et al. Up-regulation of miR-133a-3p promotes ovary insulin resistance on granulosa cells of obese PCOS patients via inhibiting PI3K/AKT signaling. BMC Womens Health. 2022;22(1):412.
36. Hernández-Jiménez JL, et al. Polycystic ovarian syndrome: signs and feedback effects of hyperandrogenism and insulin resistance. Gynecol Endocrinol. 2021;38(1):2–9.
37. Abali R, et al. Implications of circulating irisin and Fabp4 levels in patients with polycystic ovary syndrome. J Obstet Gynaecol. 2016;36(7):897–901.
38. Wang C, et al. Higher circulating irisin levels in patients with polycystic ovary syndrome:a meta-analysis. Gynecol Endocrinol. 2017;34(4):290–3.
39. Agnieszka, Adamska, et al. Serum irisin and its regulation by hyperinsulinemia in women with polycystic ovary syndrome. Endocr J. 2016;63(12):1107–12.
40. Kuai D, et al. Relationship between serum apelin, visfatin levels, and body composition in polycystic ovary syndrome patients. Eur J Obstet Gynecol Reproductive Biology. 2024;297(5):24–9.
41. Polak K, et al. New markers of insulin resistance in polycystic ovary syndrome. J Endocrinol Investig. 2016;40(1):1–8.
42. Yan B, et al. Association of serum irisin with metabolic syndrome in obese Chinese adults. PLoS ONE. 2014;9(4):e94235.
43. Chang CL, et al. Circulating Irisin and glucose-dependent insulinotropic peptide are Associated with the development of polycystic ovary syndrome. J Clin Endocrinol Metabolism. 2014;99(12):E2539–48.
44. Al-Daghri NM, et al. Irisin as a predictor of glucose metabolism in children: sexually dimorphic effects. Eur J Clin Invest. 2014;44(2):119–24.
45. Zuo C, et al. Acute and chronic functional and traditional resistance training improve muscular fitness in young males via the AMPK/PGC-1α/irisin signaling pathway. Environ Health Prev Med. 2023;28(0):69–69.
46. Butt MS, et al. Benefits of physical activity on reproductive health functions among polycystic ovarian syndrome women: a systematic review. BMC Public Health. 2023;23(1):882.
47. Gormsen LC, et al. Time-course effects of physiological free fatty acid surges on insulin sensitivity in humans. Acta Physiol. 2011;201(3):349–56.
48. McInnes KJ, et al. Regulation of Adenosine 5′,Monophosphate-Activated Protein Kinase and Lipogenesis by Androgens contributes to visceral obesity in an estrogen-deficient state. Endocrinology. 2006;147(12):5907–13.
49. Yosaee S, et al. Serum irisin levels in metabolically healthy versus metabolically unhealthy obesity: a case-control study. Med J Islam Repub Iran. 2020;34:46.
50. Cai X, et al. Circulating irisin in patients with polycystic ovary syndrome: a meta-analysis. Reprod Biomed Online. 2018;36(2):172–80.
51. Li Y et al. Cangfu Daotan Wan alleviates polycystic ovary syndrome with phlegm-dampness syndrome via disruption of the PKP3/ERCC1/MAPK axis. J Ovarian Res, 2023. 16(1).
52. Jiang XL, et al. Cangfudaotan decoction inhibits mitochondria-dependent apoptosis of granulosa cells in rats with polycystic ovarian syndrome. Front Endocrinol (Lausanne). 2022;13:962154.
53. Xiang S, et al. Effect of Electro-acupuncture on expression of IRS-1/PI3K/GLUT4 pathway in ovarian granulosa cells of infertile patients with polycystic ovary syndrome-insulin resistance of phlegm-dampness syndrome. Chin J Integr Med. 2020;27(5):330–5.
54. Flávia R. Brown adipose tissue activity is reduced in women with polycystic ovary syndrome. Eur J Endocrinol. 2019;181(5):473–80.
55. Shorakae S, et al. Brown adipose tissue thermogenesis in polycystic ovary syndrome. Clin Endocrinol. 2019;90(3):425–32.

Publisher's note